Analysis of Photothermal Release of Oligonucleotides from Hollow Gold Nanospheres by Surface Enhanced Raman Scattering (SERS)

David G. Mackanic[†], *Samuel Mabbott*[‡], *Karen Faulds*[‡], *Duncan Graham*[*,‡]

[†] Department of Chemistry, Virginia Polytechnic and State Institution, Blacksburg, Virginia 24060, United States

[‡]Centre for Molecular Nanometrology, WestCHEM, Department of Pure and Applied Chemistry, Technology and Innovation Centre, University of Strathclyde, Glasgow G1 1RD, United Kingdom

ABSTRACT: The photothermal release of single stranded DNA (ssDNA) from the surface of gold nanoparticles of different shapes and sizes is a promising mode of delivering DNA for gene-therapy applications. Here, we demonstrate the first targeted photothermal release of ssDNA from hollow gold nanospheres (HGNs) and analyse the release of the ssDNA using quantitative surface enhanced Raman scattering (SERS). The HGNs used demonstrate a tunable localized surface plasmon resonance (LSPR) frequency while maintaining size consistency, allowing for selective ssDNA release based on matching the excitation frequency to the plasmon resonance. It is shown that HGNs with resonances at 760 and HGN 670 nm release significant amounts of ssDNA when excited via 785 nm and 640 nm lasers respectively. When excited with a wavelength far from the LSPR of the particles, the ssDNA release is negligible. This is the first demonstration of SERS to analyze the amount of ssDNA photothermally released from the surface of HGNs. In contrast to traditional fluorescence measurements, this SERS based approach provides quantitatively robust data for analysis of ssDNA release and lays a strong foundation for future studies exploiting plasmonically induced ssDNA release.

1. INTRODUCTION

The development of an effective oligonucleotide delivery vector is crucial for gene therapy applications.[1] In gene therapy, therapeutic oligonucleotides target complementary DNA (antigene approach[2]) or mRNA (antisense approach[3]) sequences to inhibit protein synthesis and eliminate unwanted gene expression. Other forms of gene therapy rely on the CRISPR-Cas9 system to use engineered oligonucleotides to add new genes in the host.[4] Possible gene therapy applications include treatment of oncological,[5] inflammatory,[6] and genetic diseases such as cystic fibrosis.[7] Successful gene therapy depends on the use of an oligonucleotide delivery vector, as serum nucleases will rapidly degrade oligonucleotides released directly into the bloodstream.[8,9]

Gold nanoparticles of differing shapes and sizes have received much attention as a delivery vector for oligonucleotides due to their robust and adjustable properties.[10] Gold nanoparticles demonstrate low cytotoxicity,[11] easy cell membrane penetration,[12] and facile conjugation with a variety of therapeutic biomolecules including thiolated oligonucleotides[13] and targeting antibodies.[14] Perhaps most importantly, gold nanoparticles demonstrate significant heating upon optical excitation at the localized surface plasmon resonance (LSPR).[15,16] Photothermal heating of gold nanoparticles results in substantial temperature increase at the surface of the nanoparticles,[17] allowing for double stranded DNA (dsDNA) attached to gold nanoparticles to melt into single strands at bulk solution temperatures much lower than the melting temperature (T_m) of the dsDNA[18]. The LSPR of gold nanoparticles can be adjusted into the near infrared (NIR) region, which enables deep penetration into tissue whilst minimizing cell damage during *in vivo* treatment.

Previous work demonstrates photothermal release of oligonucleotides via denaturation of a duplex from a variety of gold nanoparticles including nanospheres[19], nanoprisms[20], nanoshells[18], and nanorods.[21] These nanoparticle systems release oligonucleotides at a specified excitation wavelength that corresponds to the LSPR of the nanoparticles. In order to improve the scope of gene therapy techniques, it is desirable to develop nanoparticle delivery systems that can sequentially and selectively release oligonucleotides[22,23] by using multiple wavelengths of lasers to excite nanoparticles with different LSPRs. Selective release of oligonucleotides from nanoparticles has been demonstrated, but the currently proposed systems suffer from various drawbacks. One drawback of the current selective oligonucleotide release system is that laser radiation induces including nanoparticle destruction.[21,24] Another major drawback is the use of vastly different sizes of gold nanoparticles to selectively release ssDNA, which may interfere with cellular uptake, limiting the ability to utilize multi-step treatment.[25,26]

In this work, we use hollow gold nanospheres (HGNs) with LSPRs of 670 nm and 760 nm to selectively release single stranded DNA (ssDNA) from a duplex upon excitation with 640 nm or 785 nm lasers. Furthermore, we demonstrate a procedure to use quantitative SERS to characterize the amount of ssDNA released through optical excitation. Quantitative SERS offers several advantages over typical methods of detecting ssDNA release from gold nanoparticles. SERS provides high sensitivity and a low detection limit, allowing for small amounts of released ssDNA to be detected.[27] Traditional fluorimeter based instruments used in ssDNA release studies are either very costly or require large amounts of ssDNA (> 1 nM) release to reach the detection limits of the instrument.[28] SERS based analysis also provides a broad spectrum of information from the released oligonucleotides, allowing the use of multivariate analysis if necessary.[29,30]

2. EXPERIMENTAL SECTION

2.1 Nanoparticle Synthesis

Unless otherwise noted, all chemicals were received from Sigma Aldrich and used without further purification. HGNs were prepared according to a previously established procedure using a sacrificial cobalt template.[31] First, 600 μL of 0.1 M sodium citrate dihydrate and 100 μL of 0.4 M cobalt chloride were added to 100 mL of DI water. After degassing the solution, 100 μL of 0.1 M sodium borohydride dissolved in degassed water was added and allowed to react for 30 min. Then, 125 μL of 0.1 M gold (III) chloride trihydrate was added to 50 mL of degassed water and added to the cobalt nanoparticles. The galvanic reaction between the gold and cobalt nanoparticles continued for 10 min before the addition of 500 μL of sodium citrate and exposure of the solution to air. Following 45 minutes of reacting with air, the solution was spun down at 5500 rpm for 35 min and re-dispersed into 10 mL of 2 mM sodium citrate. The procedure described above produces HGNs with LSPR of *ca.* 670 nm. To modify the LSPR of the HGN, different amounts of the first sodium citrate addition and gold (III) chloride trihydrate were added. To create HGN 760, 400 μL of 0.1 M sodium citrate dihydrate and 65 μL of 0.1 M gold (III) chloride trihydrate were used.

Gold nanoparticles (~30nm) were fabricated using a standard citrate-reduction reaction. First, 1 mL of 0.15 m sodium tetrachloroaurate (III) hydrate was added to 500 mL water and heated to a boil. Then, 7.5 mL of 0.025 M sodium citrate dihydrate was added and left to react while heating for 15 min. Following the heating, the solution was allowed to cool at room temperature.

2.2 Nanoparticle Conjugation with dsDNA

ssDNA was purchased from ATDbio and HPLC purified before use. The probe strand was 5' thiol modified (sequence: (5'-HS -$(HEG)_3$- CGCATTCAGGAT-3') and the target strand was fluorescently tagged at the 3' end (sequence: (5'-ATCCTGAATGCG-FAM-3')).

Conjugation of the gold nanoparticles with oligonucleotides followed a modified version of a previously reported fast-conjugation procedure.[32,33] First, HPLC purified 5' thiol-modified oligonucleotides were added in excess to the nanoparticles. Following 10 min of mixing, 3 x 20 μl aliquots of pH 2.8 citrate buffer were added in 8 min intervals. Finally, the conjugates were centrifuged at 6000 rpm for 20 min and re-dispersed in 0.1 M PBS. Following conjugation, the ssDNA on the surface was hybridized by introducing the fluorescently tagged complementary sequence in 1000 x excess. The hybridization was allowed to proceed for 1 h before centrifugation at 6500 rpm for 25 min and re-dispersion in 0.3 M PBS.

2.3 Characterization of Nanoparticles and Conjugates

All extinction spectroscopy was carried out on a Cary 300 bio UV-Visible Spectrophotometer (Varian Technologies, USA). Fluorescence data was obtained by using a Stratagene Mx3005P qPCR with the appropriate filters for FAM (Aligent, Technologies, USA). SEM was carried out on a Sirion 200 Schottky field-emission electron microscope operating at an accelerating voltage of 5 kV.

2.4 Laser Excitation and Quantitative SERS Analysis

SERS spectra were collected using a WiTec alpha300R Raman spectrometer (WiTec, Germany). In all experiments, a 532 nm variable power continuous-wave diode laser was used to probe the sample.

785nm excitation of particles utilized a high power continuous wave laser that produced a power 310 mW measured at the sample with a spot size of 3 mm (Ocean Optics, USA). 640 nm excitation utilized a 41.8 mW laser with a spot size of 1.5 mm (Innovative Photonics Solutions, USA). During laser excitation experiments, 100 μL of the NP/dsDNA solution was placed into pico centrifuge tubes. Then, the sample was mounted in the path of the laser and heating was

allowed to continue for 30 min (785 nm laser) or 60 min (640 nm laser). A control sample consisted of 100 μL of the NP/dsDNA solution placed in the dark on a table next to the laser setup. Following excitation, both samples were centrifuged at 6300 rpm for 5 min before extracting the supernatant for SERS analysis. The centrifugation and supernatant extraction serve to collect only released ssDNA while aggregating remaining NP and unreleased ssDNA. To prepare the samples for SERS, the supernatant (50 μL) was added to 50 μL of silver nanoparticles (AgNP) and mixed thoroughly. Following mixing, 15 μL of spermine was added and the solution was mixed again. The sample was immediately placed in the spectrometer and 5 spectra were collected. To normalize the spectrum for probe height and laser power, spectra were collected from 115 μL of ethanol prior to each set of measurements. The collected spectra were then normalized to the 885 cm^{-1} peak of the EtOH sample. Typical laser power used for SERS interrogation was 4.55 mW and the collection time was 3 s.

3. RESULTS AND DISCUSSION

The HGNs presented here offer several benefits as an oligonucleotide release vector. The synthesis of HGNs can be tuned to yield particles with LSPRs across a large spectrum of wavelengths ranging from 600-1100 nm. They have a controllable size and surface chemistry that is well defined based on standard thiol modifications.[34] This makes them highly attractive nanomaterial for ssDNA release. Figure 1 displays the normalized extinction spectra for a variety of HGNs created through slight alterations in the synthesis procedure. In all cases, the extinction profile is relatively narrow and demonstrates a red-shifted peak extinction value relative to spherical gold nanoparticles (AuNPs). SEM images of the HGNs confirm the monodispersity and spherical hollow shape of the particles (Figure S1).

Despite their differences in peak extinction, all of the HGNs maintain size uniformity with respect to outer shell diameter. This result is a result of different shell thicknesses of the particles and is consistent with previously reported observations.[35] When devising a sequential-release therapeutic system based on two different oligonucleotide carriers, it is important to use particles of similar size, as the size of gold nanoparticles influences both cellular uptake and response. Therefore, the pharmacokinetics of systems utilizing multiple different sizes of nanoparticles would prove nearly impossible to control.[36,37] The LSPR of HGNs depends both on the core size of the particles as well as the shell thickness. An increase in the core size creates a subsequent decrease in shell thickness while maintaining a constant outer shell diameter. Both of these size alterations red-shift the LSPR of the particles, meaning that a marginal increase in particle size creates a compounding increase in LSPR.[35] The two primary particles used in the experiments demonstrated here are 58 nm for HGN 670 and 64 nm for HGN 760 (see Table S1).

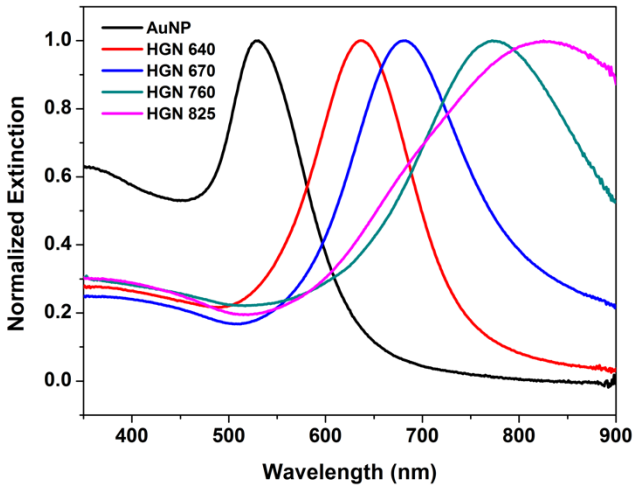

Figure 1. Normalized extinction spectra of several different HGNs and AuNPs. HGNs demonstrate tunable LSPRs that are red-shifted from AuNPs. The designations in the legend represent the peak extinction wavelength of the particles.

To demonstrate the ability of HGNs to photothermally heat upon laser excitation, laser heating experiments were conducted with two different wavelengths of laser. In all cases, AuNPs, HGN

670, and HGN 760 were tested. Prior to excitation, the peak extinction intensity of all the nanoparticles was adjusted to 0.6 (arb. units). Initially, a continuous wave, 310 mW 785 nm laser was used. The temperature of 1 mL of the bulk solution was measured every 30 s with a thermocouple placed 1 cm above the location of the laser. Figure 2 shows the thermal responses of the nanoparticles as a function of time. As expected, the particles with the LSPR closest to the excitation wavelength (HGN 760) demonstrate the strongest thermal response. Within 15 min, the temperature for HGN 760 increased by 16.9 °C, HGN 670 increased by 12.1 °C, and gold nanoparticles increased by 5.8 °C. The temperature of a similarly treated water sample increased by only 0.8 °C, indicating that the observed temperature increase of the NP samples is due to plasmonic effects. These results are similar to previously reported measurements[38] and demonstrates that the photothermal response of gold nanoparticles depends on the LSPR of the particles. A 640 nm laser was also used in this study. The 640 nm laser produces a 41.8 mW beam, which was not powerful enough to significantly heat the bulk solution and so the photothermal response of the particles was not recorded for 640 nm excitation.

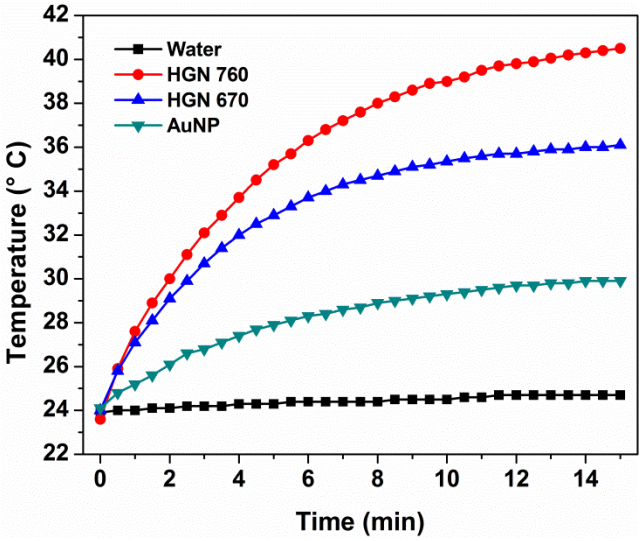

Figure 2. Photothermal response of three different types of nanoparticles upon 785nm laser excitation. The heating of the nanoparticles correlates to the proximity of their LSPR to the

excitation wavelength. Water is shown as a control, which demonstrates that almost all heating is due to nanoparticle plasmonic effects.

Following the characterization of the synthesized HGNs and confirmation of their optical properties, all nanoparticles were functionalized with hybridized oligonucleotides. The success of the conjugation was determined by observing an increase in the size of the nanoparticles as measured by a zetasizer (Malvern, UK) (Table S1). Following conjugation, the ssDNA on the surface was hybridized by introducing a fluorescently-tagged complementary sequence in 1000x excess. The procedure for functionalizing the nanoparticles did not require modification for any of the nanoparticles used.

Prior to laser excitation of the nanoparticles, the ability to thermally denature ssDNA from the surface of the particles was demonstrated through bulk heating. dsDNA-functionalized NPs were placed in a Mx3005P qPCR machine (Stratagene, USA) and heated from 25 °C to 75 °C over the course of 15 min. The release of ssDNA was monitored by measuring the increase in fluorescence of the solution. The results of this experiment are displayed in Figure S2. These results show a drastic increase in the fluorescence of the dsDNA/NP solutions at ~60 °C for all samples. The observed increase in fluorescence indicates that the NPs are functionalized with dsDNA and demonstrates the ability of these conjugates to release ssDNA upon heating. The characteristic melting point indicates that the T_m of the hybridized DNA strands is 60 °C in this experiment. Furthermore, Figure S2 shows that ssDNA release occurs over a temperature range of 40-80 °C. This temperature range and the T_m of 60 °C are higher than any temperature achieved by the laser heating shown in Figure 2. Thus, any DNA released from the NPs during laser excitation must be due to localized heating effects and not due to an increase of the bulk solution to the temperature range of thermal denaturing.

Following the confirmation of the functionalization of the nanoparticles, the conjugates were exposed to laser heating and analyzed for ssDNA release. Prior to heating, the optical absorbance of the NP conjugates was normalized to ~0.6 (a.u.). During excitation, 100 μL of conjugate solution was placed into an optical tube and positioned in the path of a laser. Three different particle types were tested: HGN 760, HGN 670, and AuNP. As in the thermal heating experiments, each set of particles was subjected to both 640 nm and 785 nm excitation. Following excitation, the samples were centrifuged and the supernatant was collected to minimize re-hybridization of the released ssDNA back to dsDNA on the nanoparticle surface. In this way, only released ssDNA in the supernatant is analyzed in the SERS measurement, while unreleased ssDNA and remaining HGN are left at the bottom of the centrifuge tube.

In this work, the release of ssDNA was analyzed with a SERS based approach that has not been demonstrated elsewhere in oligonucleotide release studies. The SERS substrate used here is spermine-aggregated AgNP, a well-known SERS substrate.[39,40] The use of spermine both aggregates the AgNP and reduces the repulsive reactions between the ssDNA and AgNPs.[41] This allows for the ssDNA to lie directly on the surface of the aggregated AgNPs, which enhances the detection of the ssDNA in solution. This procedure is a modification of a previously used technique to monitor the presence of fluoro-tagged ssDNA in solution.[41] SERS spectroscopy utilized a wavelength of 532.8 nm with a laser power of ~4.55 mW. To ensure quantitative accuracy, an ethanol standard was probed before each set of measurements. All subsequent data were collected at the same probe height and power as the EtOH standard, and were normalized to the 885 cm^{-1} peak of the ethanol spectrum upon analysis.

Excitation using the 785 nm laser occurred for 30 min, which is sufficient time to heat the nanoparticles to the excited equilibrium temperature (Figure 1). SERS spectra were collected

from both an optically excited sample and an identical "control sample" that was left in the same room as the heated sample for the duration of the excitation. When excited with a 785 nm laser, the SERs signal from the HGN 760 sample increases drastically compared to the control (Figure 3). The spectra displayed here represent the average spectra from three separate trials. This indicates the release of a significant amount of ssDNA. On the other hand, the SERS spectra from the "excited" HGN 670 and AuNP are not significantly different from the control sample. This shows that less ssDNA is released for these particle types. While a slight increase in signal is observed for both the HGN 670 and AuNP samples, this is likely due to moderate plasmonic heating effects at non-LSPR wavelengths. However, such non-LSPR effects are only observed due to the high laser power used in this experiment, as LSPR excitation is known to be the primary mode of ssDNA release in nanoparticle based systems.[10]

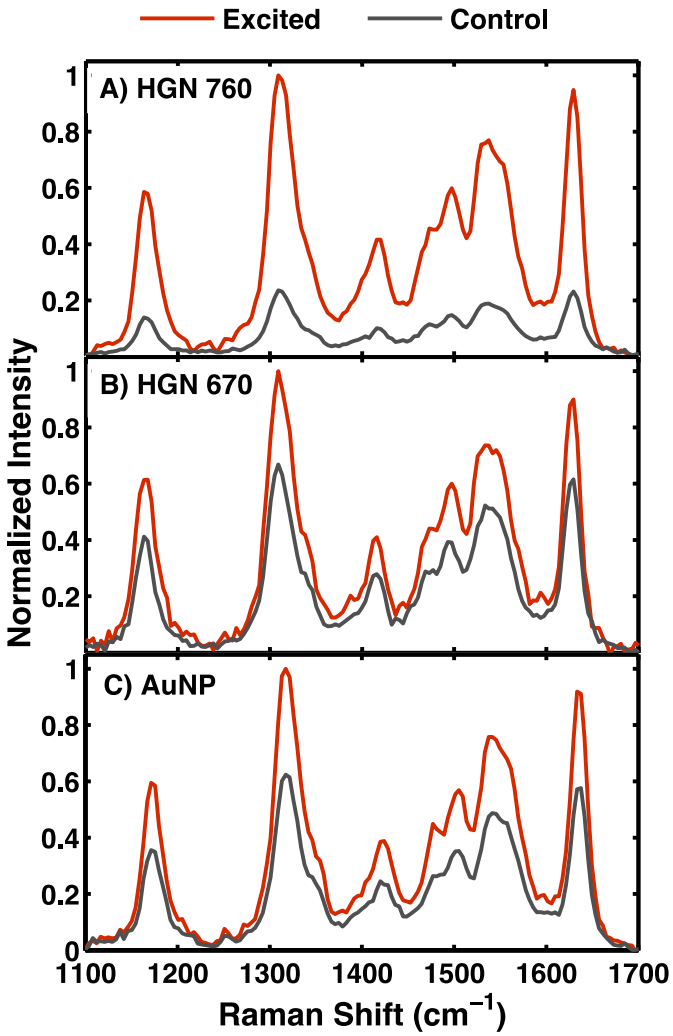

Figure 3. SERS spectra from three different nanoparticle types excited with a 785 nm laser. The red line represents SERS of optically excited samples and the gray line represents a control sample of the same HGN/dsDNA that was not excited. (A) The HGN 760 sample demonstrates a greatly increased FAM signal relative to the control, indicating ssDNA release. The change in FAM signal for the excited (B) HGN 670 and (C) AuNP samples is much smaller.

Although the 640 nm laser does not provide enough power to heat the bulk solution of the samples, excitation of the nanoparticles was conducted to see if surface plasmon effects alone could initiate DNA denaturation. In this case, each sample was heated for 1 h, and an appropriate non-excited control was used as for the 785 nm excitation. Figure 4 shows the results of exciting

the three different nanoparticle types with a 41.8 mW, 640 nm laser. These spectra represent the average spectra from three separate trials. The SERS signal for the HGN 670 sample increases significantly upon excitation from the weak 640 nm laser (Figure 4). Conversely, the change in SERS signals for the HGN 760 and AuNP samples is almost imperceptible upon excitation. The lower laser power used in this excitation precludes the non-LSPR ssDNA release observed in the 785 nm excitation experiments, as expected. This result demonstrates that localized denaturation of ssDNA can occur from metal nanoparticles without increasing the bulk temperature of the solution to the DNA melting point. This is a desirable result for therapeutic drug delivery, since low-power heating prevents excessive cell damage.

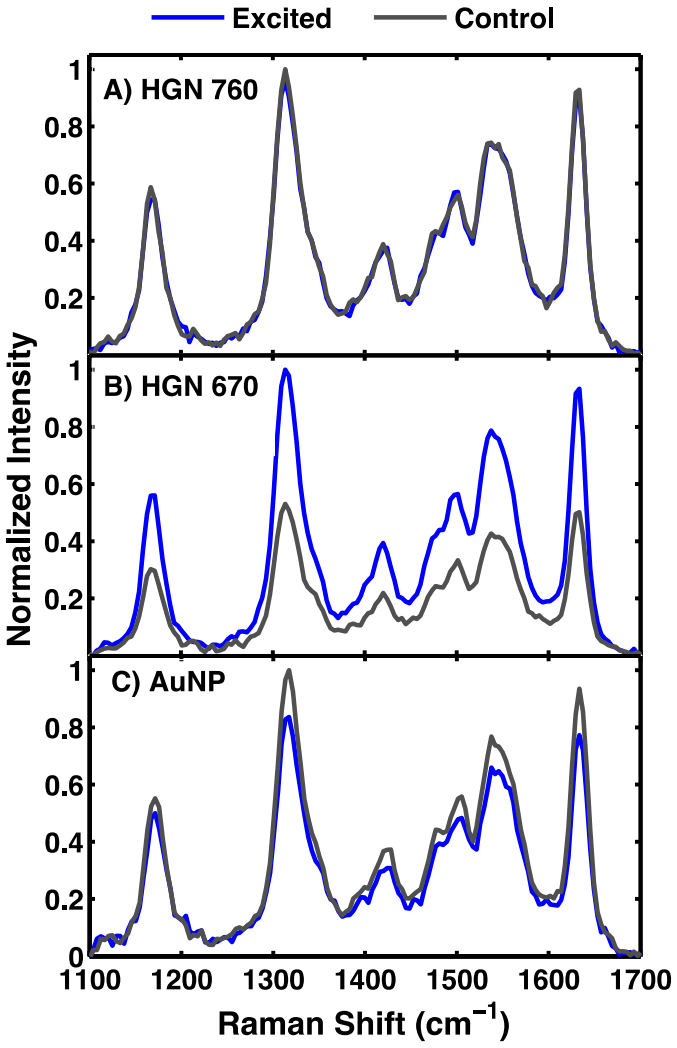

Figure 4. SERS spectra from three different nanoparticle types excited with a 640 nm laser. The blue line represents SERS of optically excited samples and the gray line represents a control sample of the same HGN/dsDNA that was not excited. (A) The SERS FAM signal for the HGN 760 samples and AuNP (C) samples scarcely change when the particles are excited. (B) The FAM signal of the HGN 670 sample increases drastically relative to a control when excited with a 640 nm laser.

A calibration curve for FAM-ssDNA was created to quantify the amount of ssDNA released from the surface of the NPs (Figure 5). To create this curve, 50 μL of various concentrations of FAM-ssDNA were added to 50 μL AgNP and 15 μL spermine. Five SERS spectra were collected for three replicates of each concentration The calibration curve was created by analyzing the height of the 1310 cm^{-1} FAM peak normalized to an ethanol standard and a 3 s collection time. The lowest concentration of ssDNA used in these experiments was 0.2 nM, and the concentration profile is linear (R^2=0.995).

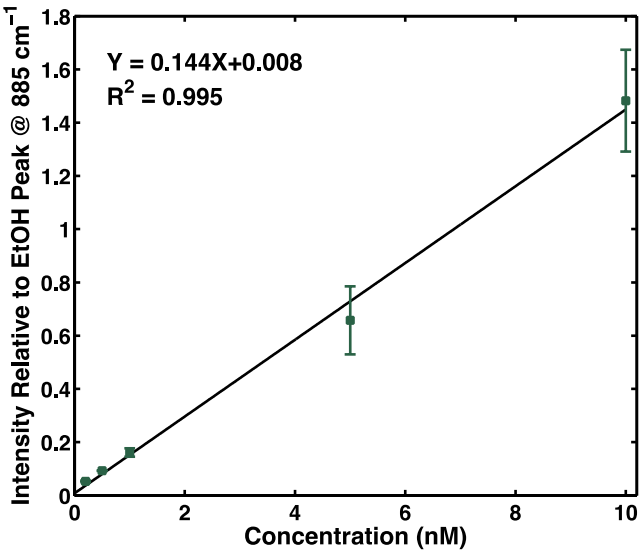

Figure 5. Calibration curve for FAM-ssDNA. The relationship between concentration and SERS peak intensity of FAM relative to an EtOH standard is strongly linear. The demonstrated detection limit is 0.2 nm.

This calibration curve was then used to determine the amounts of ssDNA released from the nanoparticles by comparing the control and excited samples for each of the excitation experiments. The difference in the peak height of the FAM signal at 1310 cm^{-1} between the excited and control sample is used to calculate the change in signal due to excitation. This intensity difference is then used with the calibration curve to determine the concentration of ssDNA released upon excitation. The quantitative results displayed in Table 1 confirm the visual observations of the SERS spectrum in Figures 3 and 4. Table 1 also displays the approximate initial concentration of ssDNA on each type of nanoparticles, calculated using the fluorimeter measurements shown in Figure S2. For 785 nm excitation, HGN 760 released nearly four times as much ssDNA as either HGN 670 or AuNP. This confirms that the LSPR of the nanoparticles influences their ability to locally denature DNA. HGN 760 release approximately 40% of the ssDNA on the particle when heated with the 785 nm laser. For 640 nm excitation, only HGN 670 demonstrates a release of ssDNA from the surface. It should be noted that the observed values of ssDNA released from HGN 760 and AuNP are negative for 640 nm excitation. It is likely that these negative values represent photobleaching of non-hybridized ssDNA during the 1 h excitation time. In this study, however, the primary interest is the drastic increase of released ssDNA for the plasmon-resonant HGN 670 particles.

Table 1. Moles of ssDNA released from different NPs upon excitation with 785 nm and 640 nm lasers.

Sample	Initial ssDNA (nM)	Released ssDNA (nM)

785 nm excitation		
HGN 760	9.23	3.59
HGN 670	8.30	0.951
AuNP	7.97	0.563
640 nm Excitation		
HGN 760	9.23	-0.073
HGN 670	8.30	1.46
AuNP	7.97	-0.305

4. CONCLUSIONS

In conclusion, selective release of ssDNA from the surface of hollow gold nanospheres is demonstrated. Excitation at a 785 nm wavelength causes significant ssDNA release from HGN 760 while causing only minor ssDNA release from HGN 670 or AuNPs. Additionally, excitation with a low-power 640 nm laser demonstrates selective melting from HGN 670 and does not release ssDNA from HGN 760 or AuNPs. The amount of DNA released in each case is quantified here using a SERS based approach, which provides a broad spectrum of data for analysis. These results indicate that ssDNA can be selectively released from NPs by tuning the LSPR of the particles to match the wavelength of excitation. Furthermore, plasmon driven DNA denaturing can occur without heating the bulk solution to the T_m of the DNA. Selective oligonucleotide release systems utilizing similarly sized nanoparticles such as this one could prove useful in therapeutic applications where multiple strands of DNA are required for localized, sequential delivery without inducing harsh in-vivo conditions. Finally, the spectroscopic techniques used to detect the amount of ssDNA released by the nanoparticles will prove useful for future studies in which small amounts of ssDNA release must be detected.

SUPPLEMENTAL MATERIAL

Figures S1 and S2, and Table S1 are available in the Supplementary Information. This material is available free of charge on the ACS Publications website.

AUTHOR INFORMATION

Corresponding Author

duncan.graham@strath.ac.uk

ACKNOWLEDGMENT

This research was conducted in the Nanometrology Lab at the University of Strathclyde under the direction of Professor Duncan Graham. DG acknowledges support from a Royal Society Wolfson Research Merit Award. This work was supported by the REU program of the National Science Foundation under award number CHE-1262908. Thanks to the American Chemical Society for coordinating the IREU exchange program.

REFERENCES

(1) Patil, S. D.; Rhodes, D. G.; Burgess, D. J. DNA-Based Therapeutics and DNA Delivery Systems: A Comprehensive Review. *AAPS J.* **2005**, *7* (1), E61–E77.

(2) Scanlon, K. J. Anti-Genes: siRNA, Ribozymes and Antisense. *Curr. Pharm. Biotechnol.* **2004**, *5* (5), 415–420.

(3) Crooke, S. T. Molecular Mechanisms of Action of Antisense Drugs. *Biochim. Biophys. Acta* **1999**, *1489* (1), 31–44.

(4) Dominguez, A. A.; Lim, W. A.; Qi, L. S. Beyond Editing: Repurposing CRISPR-Cas9 for Precision Genome Regulation and Interrogation. *Nat. Rev. Mol. Cell Biol.* **2015**, *17* (1), 5–15.

(5) Weiss, B.; Davidkova, G.; Zhou, L. W. Antisense RNA Gene Therapy for Studying and Modulating Biological Processes. *Cell. Mol. Life Sci.* **1999**, *55* (3), 334–358.

(6) Hanai, K.; Kurokawa, T.; Minakuchi, Y.; Maeda, M.; Nagahara, S.; Miyata, T.; Ochiya, T.; Sano, A. Potential of Atelocollagen-Mediated Systemic Antisense Therapeutics for

Inflammatory Disease. *Hum. Gene Ther.* **2004**, *15* (3), 263–272.

(7) Griesenbach, U.; Alton, E. W. F. W. Moving Forward: Cystic Fibrosis Gene Therapy. *Hum. Mol. Genet.* **2013**, *22* (R1), 52–58.

(8) Schubbert, R.; Lettmann, C.; Doerfler, W. Ingested Foreign (phage M13) DNA Survives Transiently in the Gastrointestinal Tract and Enters the Bloodstream of Mice. *MGG Mol. Gen. Genet.* **1994**, *242* (5), 495–504.

(9) McAllan, A. The Fate of Nucleic Acids in Ruminants. *Proc. Nutr. Soc.* **1982**, *41*, 309–317.

(10) Barhoumi, A.; Huschka, R.; Bardhan, R.; Knight, M. W.; Halas, N. J. Light-Induced Release of DNA from Plasmon-Resonant Nanoparticles: Towards Light-Controlled Gene Therapy. *Chem. Phys. Lett.* **2009**, *482* (4-6), 171–179.

(11) Connor, E. E.; Mwamuka, J.; Gole, A.; Murphy, C. J.; Wyatt, M. D. Gold Nanoparticles Are Taken up by Human Cells but Do Not Cause Acute Cytotoxicity. *Small* **2005**, *1* (3), 325–327.

(12) Van Lehn, R. C.; Ricci, M.; Silva, P. H. J.; Andreozzi, P.; Reguera, J.; Voïtchovsky, K.; Stellacci, F.; Alexander-Katz, A. Lipid Tail Protrusions Mediate the Insertion of Nanoparticles into Model Cell Membranes. *Nat. Commun.* **2014**, *5*, 4482.

(13) Love, J. C.; Estroff, L. a; Kriebel, J. K.; Nuzzo, R. G.; Whitesides, G. M. *Self-Assembled Monolayers of Thiolates on Metals as a Form of Nanotechnology.*; 2005; Vol. 105.

(14) Nam, J.-M.; Thaxton, C. S.; Mirkin, C. a. Nanoparticle-Based Bio-Bar Codes for the Ultrasensitive Detection of Proteins. *Science (80-.).* **2003**, *301* (5641), 1884–1886.

(15) Govorov, A. O.; Richardson, H. H. Generating Heat with Metal Nanoparticles We Describe Recent Studies on Photothermal Effects Using Colloidal. *Nanotoday* **2007**, *2* (1), 30–38.

(16) Haes, A. J.; Zou, S.; Schatz, G. C.; Van Duyne, R. P. Nanoscale Optical Biosensor: Short Range Distance Dependence of the Localized Surface Plasmon Resonance of Noble Metal Nanoparticles. *J. Phys. Chem. B* **2004**, *108* (22), 6961–6968.

(17) Neumann, O.; Urban, A. S.; Day, J.; Lal, S.; Nordlander, P.; Halas, N. J. Solar Vapor Generation Enabled by Nanoparticles. *ACS Nano* **2013**, *7* (1), 42–49.

(18) Huschka, R.; Zuloaga, J.; Knight, M. W.; Brown, L. V.; Nordlander, P.; Halas, N. J. Light-Induced Release of DNA from Gold Nanoparticles: Nanoshells and Nanorods. *J. Am. Chem. Soc.* **2011**, *133*, 12247–12255.

(19) Thibaudau, F. Ultrafast Photothermal Release of DNA from Gold Nanoparticles. *J. Phys. Chem. Lett.* **2012**, *3*, 902–907.

(20) Jones, M.; Millstone, J.; Giljohann, D.; Seferos, D.; Young, K.; Mirkin, C. Plasmonically Controlled Nucleic Acid Dehybridization with Gold Nanoprisms. *chemphyschem* **2009**, No. 10, 1461–1465.

(21) Wijaya, A.; Schaffer, S. B.; Pallares, I. G.; Hamad-Schifferli, K. Selective Release of Multiple DNA Oligonucleotides from Gold Nanorods. *ACS Nano* **2009**, *3* (1), 80–86.

(22) Nguyen, D.; Spitz, F.; Yen, N. Gene Therapy for Lung Cancer: Enhancement of Tumor Suppression by a Combination of Sequential Systemic Cisplatin and Adenovirus-Mediated p53 Gene Transfer. *J. Thorac. Cardiovasc. Surg.* **1996**, *112* (5), 1372–1377.

(23) Pacardo, D. B.; Ligler, F. S.; Gu, Z. Programmable Nanomedicine: Synergistic and Sequential Drug Delivery Systems. *Nanoscale* **2015**, *7* (8), 3381–3391.

(24) Fukushima, H.; Yamashita, S.; Mori, T.; Katayama, Y.; Niidome, T. Sequential Release of Single-Stranded DNAs from Gold Nanorods Triggered by Near-Infrared Light Irradiation. *Chem. Lett.* **2012**, *41* (7), 711–712.

(25) Asanuma, H.; Jiang, Z.; Ikeda, K.; Uosaki, K.; Yu, H.-Z. Selective Dehybridization of DNA-Au Nanoconjugates Using Laser Irradiation. *Phys. Chem. Chem. Phys.* **2013**, *15* (38), 15995–16000.

(26) Chithrani, B. D.; Ghazani, A. A.; Chan, W. C. W. Determining the Size and Shape Dependence of Gold Nanoparticle Uptake into Mammalian Cells. *Nano Lett.* **2006**, *6* (4), 662–668.

(27) Gracie, K.; Correa, E.; Mabbott, S.; Dougan, J. a.; Graham, D.; Goodacre, R.; Faulds, K. Simultaneous Detection and Quantification of Three Bacterial Meningitis Pathogens by SERS. *Chem. Sci.* **2014**, *5* (3), 1030.

(28) Dubus, S.; Gravel, J. F.; Le Drogoff, B.; Nobert, P.; Veres, T.; Boudreau, D. PCR-Free DNA Detection Using a Magnetic Bead-Supported Polymeric Transducer and Microelectromagnetic Traps. *Anal. Chem.* **2006**, *78* (13), 4457–4464.

(29) Feng, S.; Chen, R.; Lin, J.; Pan, J.; Chen, G.; Li, Y.; Cheng, M.; Huang, Z.; Chen, J.; Zeng Haishan, H. Nasopharyngeal Cancer Detection Based on Blood Plasma Surface-Enhanced Raman Spectroscopy and Multivariate Analysis. *Biosens. Bioelectron.* **2010**, *25* (11), 2414–2419.

(30) Rycenga, M.; Wang, Z.; Gordon, E.; Cobley, C. M.; Schwartz, A. G.; Lo, C. S.; Xia, Y. Probing the Photothermal Effect of Gold-Based Nanocages with Surface-Enhanced Raman Scattering (SERS). *Angew. Chemie - Int. Ed.* **2009**, *48* (52), 9924–9927.

(31) Xie, H.; Larmour, I. a.; Smith, W. E.; Faulds, K.; Graham, D. Surface-Enhanced Raman Scattering Investigation of Hollow Gold Nanospheres. *J. Phys. Chem. C* **2012**, *116* (14), 8338–8342.

(32) Zhang, X.; Servos, M. R.; Liu, J. Fast pH-Assisted Functionalization of Silver Nanoparticles with Monothiolated DNA. *Chem. Commun.* **2012**, *48* (81), 10114.

(33) Zaki, A.; Dave, N.; Liu, J. Amplifying the Macromolecular Crowding Effect Using Nanoparticles. *J. Am. Chem. Soc.* **2012**, *134*, 35–38.

(34) Grönbeck, H.; Curioni, A.; Andreoni, W. Thiols and Disulfides on the Au(111) Surface: The Headgroup-Gold Interaction. *J. Am. Chem. Soc.* **2000**, *122* (16), 3839–3842.

(35) Schwartzberg, A. M.; Olson, T. Y.; Talley, C. E.; Zhang, J. Z. Synthesis, Characterization, and Tunable Optical Properties of Hollow Gold Nanospheres. *J. Phys. Chem. B* **2006**, *110* (40), 19935–19944.

(36) Pan, Y.; Neuss, S.; Leifert, A.; Fischler, M.; Wen, F.; Simon, U.; Schmid, G.; Brandau, W.; Jahnen-Dechent, W. Size-Dependent Cytotoxicity of Gold Nanoparticles. *Small* **2007**, *3* (11), 1941–1949.

(37) Lin, Z.; Monteiro-Riviere, N. A.; Riviere, J. E. A Physiologically Based Pharmacokinetic Model for Polyethylene Glycol-Coated Gold Nanoparticles of Different Sizes in Adult Mice. *Nanotoxicology* **2015**, *5390* (February 2016), 1743–5390.

(38) Xie, H.; Larmour, I. a; Chen, Y.-C.; Wark, A. W.; Tileli, V.; McComb, D. W.; Faulds, K.; Graham, D. Synthesis and NIR Optical Properties of Hollow Gold Nanospheres with LSPR Greater than One Micrometer. *Nanoscale* **2013**, *5* (2), 765–771.

(39) Willets, K. a; Van Duyne, R. P. Localized Surface Plasmon Resonance Spectroscopy and Sensing. *Annu. Rev. Phys. Chem.* **2007**, *58*, 267–297.

(40) Sherry, L. J.; Chang, S.-H.; Schatz, G. C.; Van Duyne, R. P.; Wiley, B. J.; Xia, Y. Localized Surface Plasmon Resonance Spectroscopy of Single Silver Nanocubes. *Nano Lett.* **2005**, *5* (10), 2034–2038.

(41) Stokes, R. J.; Macaskill, A.; Johan Lundahl, P.; Ewen Smith, W.; Faulds, K.; Graham, D. Quantitative Enhanced Raman Scattering of Labeled DNA from Gold and Silver Nanoparticles. *Small* **2007**, *3*, 1593–1601.

TOC GRAPHICS